Relating Human Gaze and Manual Control Behavior in Preview Tracking Tasks with Spatial Occlusion

Rezunenko, Evgeny; van der El, Kasper; Pool, D.M.; van Paassen, Rene; Mulder, Max

DOI
10.1109/SMC.2018.00583

Publication date
2018

Document Version
Accepted author manuscript

Published in
Proceedings of the IEEE International Conference on Systems, Man, and Cybernetics

Relating Human Gaze and Manual Control Behavior in Preview Tracking Tasks with Spatial Occlusion

Evgeny Rezunenko, Kasper van der El, Daan M. Pool, Marinus (René) M. van Paassen, and Max Mulder
Control & Simulation section, Faculty of Aerospace Engineering
Delft University of Technology, Delft, The Netherlands
Email (corresponding author): k.vanderel@tudelft.nl

***Abstract*—In manual tracking tasks with preview of the target trajectory, humans have been modeled as dual-mode "near" and "far" viewpoint controllers. This paper investigates the physical basis of these two control mechanisms, and studies whether estimated viewpoint positions represent those parts of the previewed trajectory which humans use for control. A combination of human gaze and control data is obtained, through an experiment which compared tracking with full preview (1.5 s), occluded preview, and no preview. System identification is applied to estimate the two look-ahead time parameters of a two-viewpoint preview model. Results show that humans focus their gaze often around the model's near-viewpoint position, and seldom at the far viewpoint. Gaze measurements may augment control data for the online identification of preview control behavior, to improve personalized monitoring or shared-control systems in vehicles.**

I. Introduction

Human Controllers (HCs) can often *preview* the future target trajectory they need their vehicle to follow in manual control tasks [1], [2]. Driving is just one example, with the view of the road ahead [3]–[5]. To study how HCs use preview information for control, researchers commonly rely on laboratory tracking tasks that lack all control-related cues except the previewed trajectory [6]–[10]. Such experiments have provided evidence that HCs adopt a dual-mode control strategy [8]–[10]: open-loop *feedforward* control to track the target's *high* frequencies (fast changes) and combined *feedback-feedforward* control to follow the target's *lower* frequency components (slow changes). This dual behavior was captured in a quasi-linear HC model, with two distinct "viewpoints" on the trajectory ahead as the inputs to the two control mechanisms [8].

Together with all other model parameters, the viewpoint positions can be estimated directly from HC control data using system identification techniques. As such, a *direct* method may be available for quantifying the exact preview information ahead that a human *uses for control*. For example, in tasks with integrator Controlled Element (CE) dynamics, the near- and far-viewpoint were found to be around 0.2-0.3 s and 0.6-0.8 s ahead, respectively [9], [10]. Unfortunately, evidence for the viewpoint positions is restricted mainly to frequency-response estimates of HCs' input-output dynamics (i.e., from the displayed cues to applied manipulator deflections) [8], the interpretation of which is not unique. Additional evidence for the human's visual inputs would be highly valuable to verify that the viewpoints from [8] indeed reflect the HC's true perceptual cues. Eye-tracking measurements and spatial occlusion experiments can provide such evidence, and have already led to considerable understanding of human visual perception in many everyday tasks, like reading, sports, and driving [11]–[20].

This paper attempts to relate human *gaze* behavior to human *control* behavior in preview tracking tasks. To do so, both human gaze and control data were collected in an experiment. Gaze and control adaptations were evoked relative to a baseline tracking task with 1.5 s of full preview in three occlusion scenarios: 1) the region around the model's near viewpoint occluded (0-0.5 s), 2) the region around the far viewpoint occluded (0.35-0.85 s), and 3) zero preview, or "pursuit". The look-ahead times of the two viewpoints of the preview tracking model from [8] were estimated from the control data using system identification techniques, and were explicitly related to the recorded gaze data.

This paper is structured as follows. Section II introduces the HC preview model from [8] and discusses the visual inputs of the near- and far-viewpoint responses. It also describes the experiment, including the applied system identification, eye tracking, and spatial occlusion techniques. Results are presented in Section III, followed by a discussion in Section IV, and conclusions in Section V.

II. Methods

A. Preview Tracking and Human Gaze

1) The Control Task: In a preview tracking task, HCs must track a target trajectory $f_t(t)$, see Fig. 1, which is visible up to a preview time τ_p s ahead. The previewed trajectory $f_t([t, t+\tau_p])$ moves over the display screen from right to left, forcing the current target marker ("+" in Fig. 1) to move vertically. The HC provides control inputs $u(t)$ to the CE to guide its output $x(t)$ ("○" in Fig. 1, restricted to vertical movements) over the target trajectory, minimizing the tracking error $e(t) = f_t(t) - x(t)$. In this paper, the CE has integrator dynamics and is perturbed vertically by a disturbance $f_d(t)$. This combined target-tracking and disturbance-rejection, velocity control task is similar as in [8]–[10].

2) Preview Control Model: Fig. 2 shows the quasi-linear HC model for preview tracking tasks from [8]. This model has been shown to accurately describe measurements of HC multiloop response dynamics in tasks with a range of controlled element dynamics [9] and preview times [10]. The model's inner-loop resembles McRuer's crossover model [21]. HC use

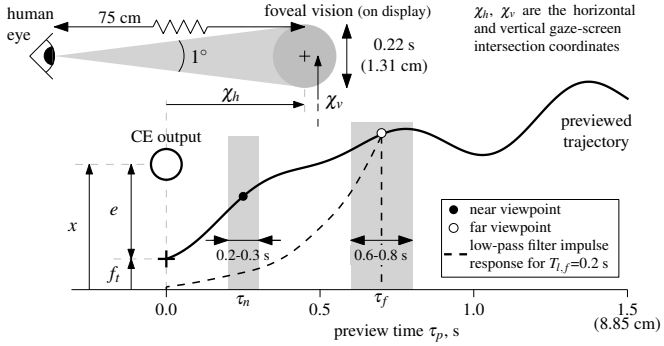

Fig. 1. Preview tracking display with approximate regions of the near- and far-viewpoint locations in gray [9], [10]. Image is drawn to scale to indicate the part of the previewed trajectory that falls onto the eye's foveola, at 75 cm viewing distance (corresponding to the experimental setup in [9], [10]).

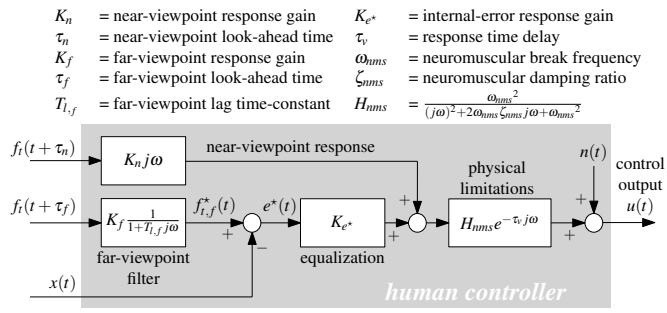

Fig. 2. Quasi-linear human controller model for preview tracking tasks with integrator controlled element dynamics [8]. The near-viewpoint response dynamics are simplified, in accordance with [9].

of preview is accounted for with two additional responses that are based on a near- and a far-viewpoint, positioned τ_n and τ_f s ahead on the previewed trajectory, respectively (see also Fig. 1). The far viewpoint is the input to the compensatory inner-loop, and is the primary means through which HCs use preview. However, whereas the true error $e(t)$ is minimized in compensatory tasks, $e^\star(t)$ in preview tasks is an *internally calculated*, *time-advanced* error between the CE output and target τ_f s ahead, pre-shaped by the far-viewpoint filter (see Fig. 2). As such, HCs smoothly track only the lower frequencies (slow changes) of the target with the far-viewpoint response. Some HCs also track higher frequencies in the target signal by mechanizing a second, open-loop feedforward response based on a near viewpoint (Fig. 2); this response is relatively weak compared to the far-viewpoint response [9].

3) Human Gaze: The preview model in Fig. 2 suggests that HCs use three explicit visual inputs: the CE output $x(t)$, the near viewpoint $f_t(t+\tau_n)$, and the far viewpoint $f_t(t+\tau_f)$. These are drawn to scale in Fig. 1, together with the area that can be captured by the eye's foveola, that is, a one deg visual angle around the HC's gaze direction [14], [16], [22] (referred to as foveal vision in this paper). Fig. 1 illustrates that foveal vision cannot sample the three model inputs simultaneously, suggesting that HCs periodically move their gaze between the three inputs, sampling each with foveal vision on average one third of the time. Alternatively, at least two model inputs may be perceived with extrafoveal vision, yielding reduced spatial perception accuracy, because visual acuity outside the eye's foveala decreases, to a 50% acuity at the outer edge of the visual angle that covers all three model inputs (≈4 deg) [14].

B. Hypotheses

Because HCs need to sample both model viewpoints to track a previewed trajectory, we hypothesize that the model's viewpoint positions (τ_n and τ_f) correlate with the average *horizontal* HC gaze location χ_h (see Fig. 1), and viewpoint adaptations are accompanied by equivalent gaze adaptations (H.I.). Second, we hypothesize that the *vertical* HC gaze location χ_v is correlated mostly with the target, and not the CE output, as suggested in previous work on eye-tracking [23] and car driving [12], [24] (H.II). We performed a human-in-the-loop experiment to test these hypotheses.

C. Experiment Design

1) Independent Variables: The experiment had four conditions, which are shown in Fig. 3. In the baseline condition, 1.5 s full preview (PR) of the trajectory was visible. Gaze and control behavior adaptations were evoked in three additional conditions, by occluding either a 0.5 s long portion of the previewed trajectory around the near-viewpoint (NO), a 0.5 s portion around the far viewpoint (FO), or all of the previewed trajectory, yielding a pursuit (PS) tracking task.

2) Apparatus: Fig. 4 shows the experimental simulator. Subjects gave control inputs $u(t)$ with an electro-hydraulic side-stick (Fig. 4d), which rotated only around the pitch axis; pitching the stick backwards moved the CE up and *vice versa*. A non-intrusive, remote head- and eye-tracker (faceLAB Seeing Machines, version 4.3.0) was used to measure the gaze-screen intersection position. Fig. 4 shows the eye-tracker's three infrared pods (a) positioned in a triangular shape around the display screen (c) to create reflections in the subjects' eyes, which where then measured by two cameras (b).

3) Subjects and Experimental Procedure: Eight subjects participated; they were instructed to minimize the tracking error $e(t)$. Each subject was first familiarized with the task, by consecutively performing three PS, seven PR, two NO, and two FO runs. This rather long familiarization phase was indispensable, because it was not directly evident for our subjects how to "optimally use" the remaining visible preview in the occlusion scenarios. Additionally, subjects needed time to find a comfortable seating position, before the eye-tracking equipment was calibrated ("precision gaze" setting) for the measurements. Next, subjects performed a single condition until performance was stable in at least five runs, which were used as data for analysis. The order of the four conditions was randomized according to a balanced Latin-square.

The first 8 s of each 128 s long run were used as run-in time; the last 120 s were analyzed. Time-traces of the error $e(t)$, the CE output $x(t)$, and the stick deflections $u(t)$ were recorded at 100 Hz. The horizontal and vertical positions where subjects' gazes intersected with the display screen, $\chi_h(t)$ and $\chi_v(t)$, respectively, were logged synchronously.

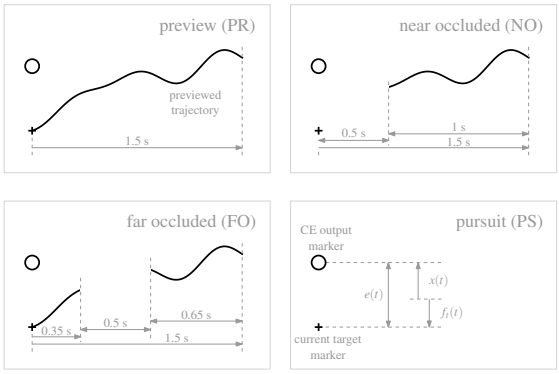

Fig. 3. The four experimental displays, drawn to scale; only the black indicators and the winding previewed trajectory were visible to the subjects.

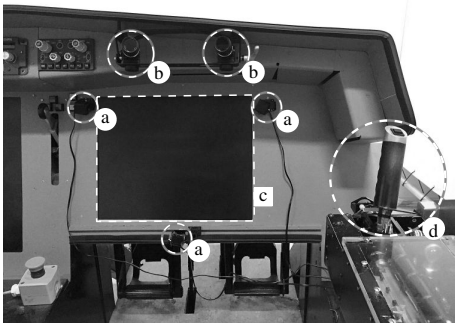

Fig. 4. Experimental apparatus viewed from the subjects' perspective during the experiment. The eye-tracker hardware consists of three infrared pods (a) and two cameras (b). The preview display was presented on the central screen (c), and control inputs were given with the side-stick (d).

D. Data Analysis

1) Tracking Performance and Control Activity: The variance of the tracking error σ_e^2 was used as performance measure, and was calculated per run by integrating the error signal's power spectrum [9]. Individual contributions of the target and disturbance signal to the total tracking error were estimated by integrating only over each signal's respective input frequencies [9]; integrating over the remaining frequencies yielded the remnant contribution. These estimates ignore the small remnant contribution at the target and disturbance input frequencies. The control output variance σ_u^2 was calculated similarly and was used as control activity measure.

2) Gaze Positions: Distributions of *horizontal* gaze positions on the screen $\chi_h(t)$ were used as measure for the visual regions of interest along the previewed trajectory. These distributions were further quantified with their medians $\tau_{\chi_h^{med}}$ and inter-quartile ranges $\tau_{\chi_h^{iqr}}$. Gaze measurements were first filtered by removing the data points where subjects' eyes were (nearly) closed and where the measured gaze was outside the screen area (Fig. 4c). The horizontal gaze positions were scaled to seconds of preview and compensated with the eye tracker's bias, which was estimated per subject in the pursuit condition as the difference between $\tau_{\chi_h^{med}}$ and τ=0 s (the position of the CE and current-target markers, see Fig. 1).

Time traces of the *vertical* gaze positions $\chi_v(t)$ were used as measure for the synchronousness of the vertical gaze with the target and CE output signals. These were further quantified with the time shifts (τ_{χ_v,f_t} and $\tau_{\chi_v,x}$) that maximizes their cross-correlation function R, similar as in [23]:

$$R_{\chi_v,f_t}(\tau) = \int_{-\infty}^{\infty} \chi_v(t) f_t(t+\tau)\,\mathrm{d}t \tag{1}$$

The cross-correlation between the CE output and the vertical gaze position $R_{\chi_v,x}$ is defined similarly. Before computing R, the vertical gaze position data were first interpolated to a constant 100 Hz sampling frequency using shape-preserving piecewise cubic interpolation. Next, these data were smoothed using non-causal frequency-domain filtering, by explicitly setting the power at all frequencies higher than 16 rad/s (above the highest forcing function input frequency) to zero.

3) HC control Behavior: The model parameter vector $[K_n\ \tau_n\ K_f\ T_{l,f}\ \tau_f\ K_{e^\star}\ \omega_{nms}\ \zeta_{nms}\ \tau_v]^T$ was estimated by minimizing the least-squares errors between the Fourier transforms of the modeled and measured $u(t)$, identical to [8]–[10]. In this paper only the look-ahead times τ_n and τ_f will be discussed.

4) Statistical Analyses: For each dependent measure, the PS, NO, and FO conditions were individually compared to the PR condition. If the data in any of the two compared condition violated the Lilliefors normality test ($p<.05$), a Wilcoxon signed-rank test was performed, otherwise a paired-sample t-test was used. Bonferroni corrections were applied for the three comparisons, with the significance level set to $p<.0167$.

III. Results

A. Tracking Performance and Control Activity

Fig. 5a shows that full preview yields superior performance (low total σ_e^2). Performance significantly deteriorates for the pursuit task, mostly due to a higher error at the target input frequencies (white portion of the bar). Both occlusion scenarios (NO and FO) yield worse total performance than full preview, due to contributions of the target and disturbance.

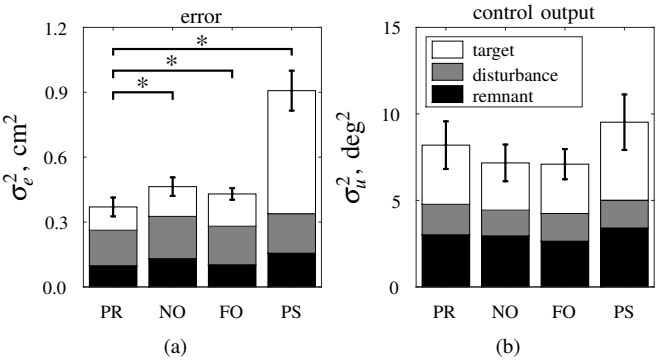

Fig. 5. Mean variances of the error (a) and control input (b) of the eight subjects, at the target, disturbance, and remnant frequencies. Errorbars indicate the 95% confidence intervals on the total, compensated for between-subject variability; significant total effects relative to PR are indicated by a "$*$".

Pursuit evokes a slightly higher control activity than full preview, see Fig. 5b, especially at the target input frequencies. Both occlusion scenarios show consistently lower control activity than the full preview condition, but these effects are not statistically significant.

B. Eye-Tracking Results

1) Horizontal Gaze: Fig. 6 shows the distributions of the measured horizontal gaze positions on the screen, along the previewed trajectory; Fig. 7 shows their medians and inter-quartile ranges. In the pursuit condition (PS, Fig. 6d), the median of each subject's distribution is exactly at τ=0 s, because we compensated the gaze data with the bias measured in this condition. The inter-quartile range reflects the combined noise of the eye-tracking measurement equipment and oculomotor "variability", due to nystagmus, drifts, and microsaccades [13].

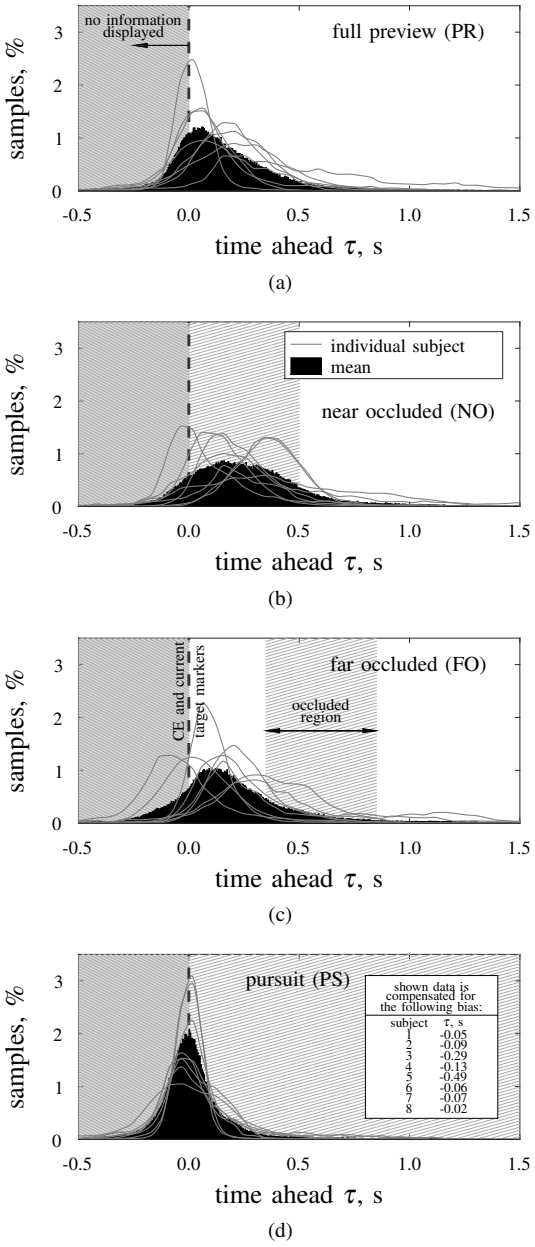

Fig. 6. Horizontal gaze position distributions, based on 1 pix. (0.0048 s) bins, in preview (a), near-occluded (b), far-occluded (c), and pursuit (d) conditions.

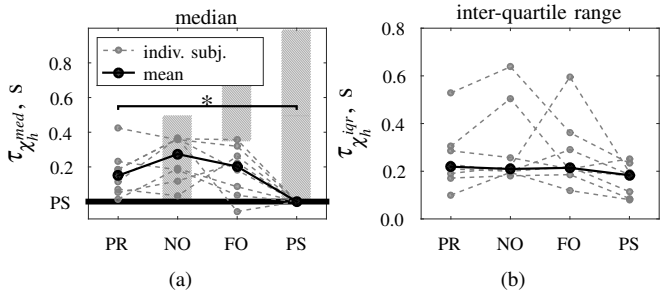

Fig. 7. Horizontal gaze distribution median (a) and inter-quartile range (b).

With full preview (PR) the median gaze position shifts to approximately 0.15 s ahead, see Fig. 7a, which is significantly different from the pursuit condition. The inter-quartile range is only slightly higher with full preview (not significant), indicating that subjects focused their gaze roughly on the same point ahead throughout the measurement runs, and rarely shifted their gaze to other trajectory parts. The positive skew of the mean distribution in Fig. 6a reflects the between-subject spread of visual attention along the previewed trajectory.

When the near preview region is occluded (NO), subjects generally focus their gaze farther ahead than with full preview, see Fig. 7a. However, the distribution median is not significantly different. The inter-quartile range is identical as in full preview tasks, and Fig. 6b shows that the gaze is most of the time focused directly *into* the occluded region (0-0.5 s ahead). Apparently, subjects try to simultaneously observe the CE marker at τ=0 s (required for disturbance rejection), and the previewed trajectory ahead at τ>0.5 s (target trajectory anticipation), without focusing their gaze on either point.

Occluding the far preview region (FO) yields distribution medians and inter-quartile ranges that are identical to the PR condition. Nonetheless, the wider spread of the distributions' medians in Fig. 7a *between subjects* relative to full preview suggests that individuals adapt their gaze differently. Fig. 6c shows that the gaze is often focused on the part of the previewed trajectory before (τ<0.35 s) and seldom beyond (τ>0.85 s) the occluded region.

It must be noted that the measured horizontal gaze positions suffered from some drift throughout the experiment, likely due to subject posture changes. An example is the single gaze median that is to the left of the CE and target markers (τ<0 s, Fig. 7a, FO), where in fact no information is shown on the screen. These biases on average cancel out between subjects (partly due to the experiment's balanced Latin-square design), hence they do not affect our main findings.

2) Vertical Gaze: Fig. 8 shows time-traces of a representative sample of the vertical gaze and CE output positions relative to the target trajectory. Both the CE output and the vertical gaze clearly lag behind the target signal in pursuit tasks, but these lags disappear with preview.

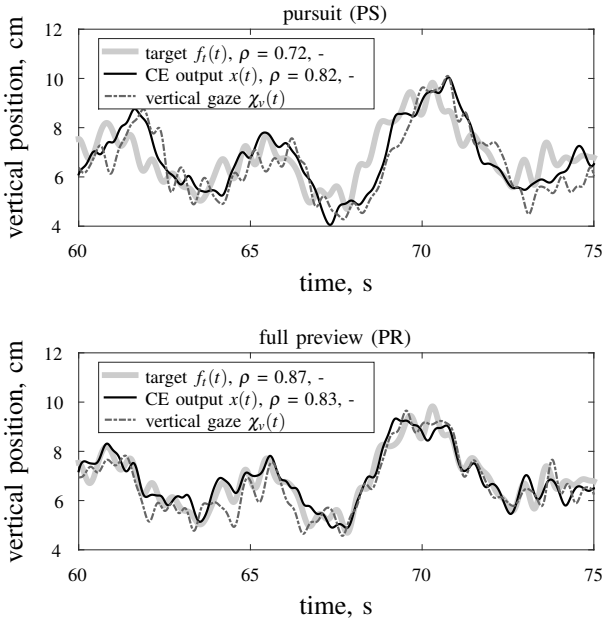

Fig. 8. Vertical gaze position, target, and CE output time-traces from a run where the gaze data were relatively low noise. The Pearson correlation coefficients ρ indicate the signals' correlation with the vertical gaze position.

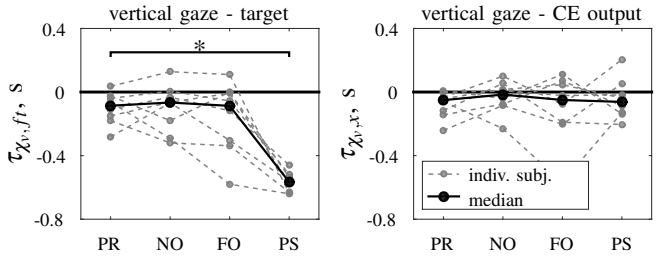

Fig. 9. Time shifts τ that maximize the cross-correlation function $R(\tau)$ between the vertical gaze and the target and the CE output signals.

Fig. 9 shows the time shifts that maximize the cross-correlation function R (i.e., the correlation coefficient ρ in Fig. 8). In the pursuit condition, the vertical gaze lags the target and CE output signals by approximately 0.5 and 0.05 s, respectively, which indicates that subjects focus their gaze mainly on the CE output and not on the target. The gaze signal's lag on the target signal reduces to 0.1 s with preview (significant effect), while the lag relative to the CE remains constant at 0.05 s. The vertical gaze data thus suggest that subjects focus their attention mainly on the CE output marker's vertical motions and not on the (future) target trajectory.

C. Estimated Near- and Far-Viewpoint Positions

Fig. 10 shows the estimated near- and far-viewpoint positions, corresponding to the model's look-ahead time parameters τ_n and τ_f, respectively. With full preview, subjects position their near- and far-viewpoints around 0.25 and 0.8 s ahead, respectively. The occluded regions in the NO (0-0.5 s) and FO (0.35-0.85 s) conditions thus indeed obscured the intended

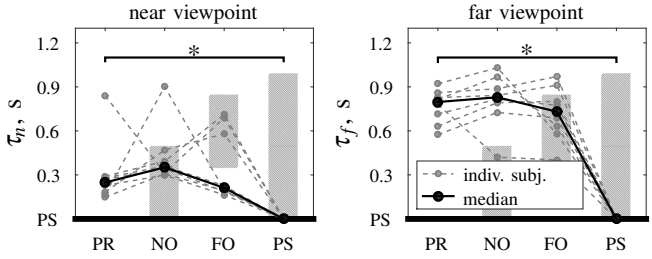

Fig. 10. Estimated near- (τ_n) and far-viewpoint (τ_f) positions on the previewed trajectory ahead.

parts of the trajectory from the subjects' view. Several outliers are visible in τ_n, indicating that these subjects initiated no (or a very weak) near-viewpoint response [9].

Occluding the near preview region (NO) leads the *near*-viewpoint to move slightly farther ahead along the trajectory (not significant). It is estimated to be positioned *within* the occluded region, similar to subjects' horizontal gaze, Fig. 6b. Near occlusion does *not* impact the *far*-viewpoint position.

Occluding the far region (FO) motivated several subjects to move their far viewpoint substantially *closer* ahead, whereas others move it *farther* ahead. This is consistent with the observed wider variety in gaze strategies (see Fig. 7) and suggests that finding the "optimal" strategy is not evident. For most subjects the far viewpoint is positioned inside the occluded region. More subjects (3) than in any other condition initiate no (or a very weak) near-viewpoint response. Moreover, despite that far occlusion does not hide the near viewpoint, subjects position their near viewpoint slightly closer ahead compared to the PR condition (not significant). Tentatively, the far preview region, beyond 0.35 s ahead, contains essential information about the target signal's high-frequency oscillations, on which near-viewpoint response relies.

IV. Discussion

Our first hypothesis was that adaptations of gaze and model viewpoint positions are related. Fig. 11 shows the correlations of these parameters. Whereas the gaze median and viewpoint positions are by definition at τ=0 s in pursuit tasks, both are clearly nonzero in preview tasks, indicating that HCs both respond to and focus their gaze on the trajectory ahead. This confirms our first hypothesis H.I. Fig. 11 also shows that the horizontal gaze position median correlates very well with the *near*-viewpoint position. HCs seldom aim their gaze at the far viewpoint ($\approx$0.8 s), which is positioned considerably beyond the third quartile of the gaze distribution ($\approx$0.4 s, Fig. 11).

Tentatively, the predominant visual attention on the near region is indispensable for HCs to *recognize* the high-frequency target trajectory oscillations, required to mechanize the *open-loop* near-viewpoint response. Moreover, substantial visual attention is drawn to the CE output marker (at τ=0 s), the movement of which provides the *only* information about the external disturbance signal f_d. HCs in general aim their gaze *vertically* at the CE output marker (Fig. 9), and not at the

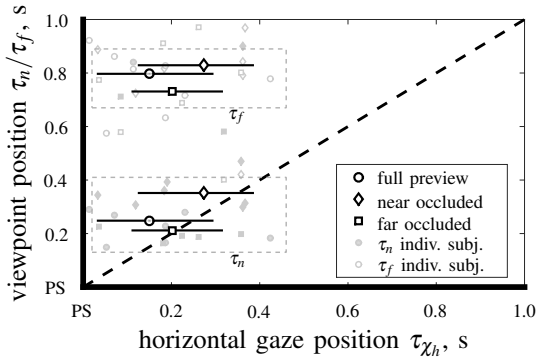

Fig. 11. Correlation between horizontal gaze and near- and far-viewpoint positions. Data correspond to Figs. 7 and 10, errorbars on horizontal gaze positions indicate the distributions' inter-quartile ranges.

target, opposed to tasks that lack an external disturbance [23], [24]; our second hypothesis (H.II) is thus *not* confirmed. Note, however, that the CE marker is often very close to the near viewpoint, and both can be sampled simultaneously with foveal vision. HCs' visual attention can be expected to shift towards the far viewpoint in other control tasks where: 1) no explicit information is obtained from the CE output marker (e.g., "inside-out" viewing perspective in driving [24]), and 2) no near-viewpoint response is initiated (e.g., following a low-frequency target trajectory with a double integrator CE [9]).

Contrary to our expectations, viewpoint and gaze positions did not fully shift to a visible part of the previewed trajectory in the occlusion scenarios. HCs seem to resist adapting their behavior to occlusion. This lack of adaptation may be explained by the invariance of the "perfect" target-tracking dynamics, which HCs were shown to match well with full preview [9], [10]. Viewpoint positions outside the occluded regions would be suboptimal and yield inferior performance. To still respond to the "optimal" viewpoints, HCs likely use a part of the trajectory beyond the occluded region to estimated the target values at the viewpoints.

Future work can focus on how to relate gaze data with model viewpoints. Task variables, such as the CE dynamics are likely to affect the model's viewpoints [9], but it is unknown whether HCs also adapt their gaze. Note that to truly "connect" human gaze to control behavior, a time-*varying* relation between gaze and model viewpoints must be found, rather than the time-*averaging* approach adopted here [2].

V. Conclusion

A unique combination of gaze and control-behavioral data is presented, obtained in a preview tracking experiment, which improves our understanding of the (visual inputs of) humans' near- and far-viewpoint responses. Results indicate that humans focus their gaze predominantly around the model's near-viewpoint position, and seldom at the far viewpoint. Establishing the relation between gaze and control behavior in a wide range of tasks may increase the implications drawn from future eye-tracking measurements, and facilitate the (online) identification of preview control behavior from gaze data.

References

[1] T. B. Sheridan, "Three models of preview control," *IEEE Trans. on Human Factors in Electronics*, vol. 7, no. 2, pp. 91–102, Jun. 1966.

[2] M. Mulder, D. M. Pool, D. A. Abbink, E. R. Boer, P. M. T. Zaal, F. M. Drop, K. van der El, and M. M. van Paassen, "Manual Control Cybernetics: State-of-the-Art and Current Trends," *IEEE Trans. on Human-Machine Systems*, 2018.

[3] C. C. MacAdam, "Application of an optimal preview control for simulation of closed-loop automobile driving," *IEEE Trans. on Systems, Man, and Cybernetics*, vol. 11, no. 6, pp. 393–399, Jun. 1981.

[4] R. A. Hess and A. Modjtahedzadeh, "A control theoretic model of driver steering behavior," *IEEE Control Systems Magazine*, vol. 10, no. 5, pp. 3–8, 1990.

[5] S. D. Keen and D. J. Cole, "Bias-free identification of a linear model-predictive steering controller from measured driver steering behavior," *IEEE Trans. on Systems, Man, and Cybernetics, Part B: Cybernetics*, vol. 42, no. 2, pp. 434–443, Apr. 2012.

[6] K. Ito and M. Ito, "Tracking behavior of human operators in preview control systems," *Electrical Eng. in Japan*, vol. 95, no. 1, pp. 120–127, 1975, (Transl.: D.K. Ronbunshi, vol. 95C, no. 2, Feb. 1975, pp 30-36).

[7] M. Tomizuka and D. E. Whitney, "The human operator in manual preview tracking (an experiment and its modeling via optimal control)," *J. Dynamic Systems, Measurement, and Control*, vol. 98, no. 4, pp. 407–413, Dec. 1976.

[8] K. van der El, D. M. Pool, H. J. Damveld, M. M. van Paassen, and M. Mulder, "An empirical human controller model for preview tracking tasks," *IEEE Trans. on Cybernetics*, vol. 46, no. 11, pp. 2609–2621, Nov. 2016.

[9] K. van der El, D. M. Pool, M. M. van Paassen, and M. Mulder, "Effects of preview on human control behavior in tracking tasks with various controlled elements," *IEEE Trans. on Cybernetics*, vol. 48, no. 4, pp. 1242–1252, Apr. 2018.

[10] K. van der El, S. Padmos, D. M. Pool, M. M. van Paassen, and M. Mulder, "Effects of preview time in manual tracking tasks," *IEEE Trans. on Human-Machine Systems*, 2017, accepted.

[11] D. A. Gordon, "Perceptual basis of vehicular guidance: IV," *Public Roads*, vol. 34, no. 3, pp. 53–68, 1966.

[12] M. F. Land and D. N. Lee, "Where we look when we steer," *Nature*, vol. 369, pp. 742–744, Jun. 1994.

[13] K. Rayner, "Eye movements in reading and information processing: 20 years of research," *Psychol. Bull.*, vol. 124, no. 3, pp. 372–422, 1998.

[14] M. F. Land, "Eye movements and the control of actions in everyday life," *Progress in Retinal and Eye Research*, vol. 25, pp. 296–324, 2006.

[15] D. Panchuk and J. N. Vickers, "Using spatial occlusion to explore the control strategies used in rapid interceptive actions: Predictive or prospective control?" *Journal of Sports Sciences*, vol. 27, no. 12, pp. 1249–1260, Oct. 2009.

[16] H. Strasburger, I. Rentschler, and M. Juttner, "Peripheral vision and pattern recognition: A review," *Journal of Vision*, vol. 11, no. 13, pp. 1–82, 2011.

[17] E. R. Schotter, B. Angele, and K. Rayner, "Parafoveal processing in reading," *Attention, Perception and Psychophysics*, no. 74, pp. 5–35, 2012.

[18] P. M. van Leeuwen, R. Happee, and J. C. F. de Winter, "Vertical field of view restriction in driver training: A simulator-based evaluation," *Transportation Research Part F: Traffic Psychology and Behaviour*, vol. 24, pp. 169–182, May 2014.

[19] D. C. Niehorster, W. W. F. Siu, and L. Li, "Manual tracking enhances smooth pursuit eye movements," *Journal of Vision*, vol. 15, no. 11, pp. 1–14, 2015.

[20] R. Zheng, K. Nakano, H. Ishiko, K. Hagita, M. Kihira, and T. Yokozeki, "Eye-gaze tracking analysis of driver behavior while interacting with navigation systems in an urban area," *IEEE Trans. on Human-Machine Systems*, vol. 46, no. 4, pp. 546–556, Dec. 2016.

[21] D. T. McRuer and H. R. Jex, "A review of quasi-linear pilot models," *IEEE Trans. on Hum. F. in Electr.*, vol. 8, no. 3, pp. 231–249, 1967.

[22] B. A. Wandell, *Foundations of Vision*, 1st ed. Sinauer Ass. Inc., 1995.

[23] T. A. Bahill and J. D. McDonald, "Smooth pursuit eye movements in response to predictable target motions," *Vision Research*, vol. 23, no. 12, pp. 1573–1583, 1983.

[24] J. P. Wann and D. Swapp, "Why you should look where you are going," *Nature Neuroscience*, vol. 3, no. 7, pp. 647–648, Jul. 2000.